

# Parametric Optimization of Inkjet Printing and Optical Sintering of Nanoparticle Inks

Erja Sipilä<sup>1</sup>, Yanan Ren<sup>1</sup>, Johanna Virkki<sup>1</sup>, Lauri Sydänheimo<sup>1</sup>, Manos M. Tentzeris<sup>2</sup>, and Leena Ukkonen<sup>1</sup>

<sup>1</sup>Department of Electronics and Communications Engineering, Tampere University of Technology, Tampere, Finland

<sup>2</sup>School of Electrical and Computer Engineering, Georgia Institute of Technology, Atlanta, USA

**Abstract**—In this paper, the parameters for inkjet-printing and photonic sintering of silver and copper nanoparticle inks on flexible polyimide substrate were studied by manufacturing simple line patterns. The results were then utilized to manufacture passive ultra high frequency (UHF) radio frequency identification (RFID) tag antennas on polyimide substrate. The tag's performance was evaluated by wireless measurements. Tags achieved peak read ranges of 3.6–5.5 meters, which can be considered suitable for practical applications.

**Index Terms**—inkjet printing, photonic sintering, RFID, UHF, tag, antenna, nanoparticle ink.

## I. INTRODUCTION

Passive ultra high frequency (UHF) radio frequency identification (RFID) tags are seen as the key enablers of the Internet of Things (IOT), a conceptual vision to connect people, things and devices and create a ubiquitous computing world. In order to connect everyday objects to large networks, this kind of simple, reliable, and cost-effective technology is crucial.

Currently the most commonly used method for fabricating RFID tag antennas in mass production is etching. Besides for etching being a subtractive method, it needs lots of environmentally harmful chemicals. Thus, the use of additive manufacturing methods, such as printable electronics, is a growing trend. In additive manufacturing, the materials are added only to locations where they are needed, thus significantly decreasing waste compared to traditional manufacturing methods. Great potential lies, e.g., in use of wood, fabric, and flexible materials, such as polyimide, as a substrate for RFID components. Inkjet printing can also allow tags to be printed directly onto product packages. These RFID components can be used, e.g., in intelligent transportation, logistics, and healthcare applications.

Inkjet printing of RFID tags using silver nanoparticle ink and heat sintering has been successfully studied, e.g., in [1-3]. The main limitations of this method are the high cost of silver nanoparticle ink and the long heat sintering time. Especially the long sintering time prevents the use of this manufacturing technology in mass production.

The substrate material plays a big role in additive RFID tag manufacturing. Different substrate materials need different printing parameters, because they have different surface properties and morphologies. In addition, the substrate material

has to withstand the sintering process, e.g., high temperature in heat sintering. Naturally, the substrate material should be cost-effective and preferably also flexible.

For RFID technology to spread to new application areas in the IOT, the manufacturing methods and materials for RFID tag antenna manufacturing have to be optimized. This also means that effective and optimized sintering methods are needed. Flash lamp sintering is a photonic sintering method that in ambient conditions uses short light pulses from a flash lamp to heat the ink to a high enough temperature within milliseconds. Such transient heating minimizes the damage to sensitive substrates [4] and enables roll-to-roll mass production. In addition, it allows cheaper ink alternatives, e.g., copper nanoparticle ink, to be used, because the sintering method reduces significantly the problem of non-conductive copper oxide formation.

In this study, to efficiently manufacture inkjet-printed passive UHF RFID tag antennas, we first optimized the manufacturing parameters for inkjet printing and photonic sintering of silver and copper nanoparticle inks on polyimide substrate. The optimized manufacturing parameters were used to fabricate prototype UHF RFID tags and the tags were evaluated by wireless measurements.

## II. PHOTONIC SINTERING

Manufacture of inkjet-printed conductive structures consists of two steps: inkjet-printing of the desired pattern with nanoparticle ink and metallization of it by sintering. Several different sintering techniques are available, such as laser, microwave, plasma, and electrical sintering, as well as sintering by chemical agents. Each solution naturally comes with different restrictions and shortcomings. In case of copper inks, heat sintering is not easy because of non-conductive copper oxide; a copper ink needs an inert atmosphere or an alternative approach to sintering. Thus, the best alternative to thermal sintering process is an active research area [5]. Perhaps the most promising method, especially when considering low-cost mass-production, is the photonic sintering method with a Xenon flash lamp.

The idea in photonic sintering is to transfer energy via light radiation to conductive particles so fast, within micro- or milliseconds, that the conductive particles heat enough to sinter before they transfer too much of heat energy to the

substrate [6]. In addition, the very short sintering time prevents oxidation of copper nanoparticles during photonic sintering process [4].

In this study, the inkjet-printed patterns were sintered using Xenon Sinteron 2010-L system [7], which is presented in Fig.1. The sintering system parameters are lamp voltage, pulse duration, and flash number (single, double, continuous or burst). The lamp voltage can be adjusted between 1800 V and 3000 V, in 50 V increments. The pulse duration can be adjusted (min 100  $\mu$ s, max 2000  $\mu$ s), as can the time period (the time period includes the pulse and the time between the pulses). The minimum time period is 100 ms and maximum is 5000 ms. In burst mode, the sintering system will count the flashes, and the count number can be adjusted (min 1, max 2000). In addition, there are two plates that can be used to shape the light into a stripe that hits the sample. This aperture spacing can be adjusted from 10 mm to 80 mm. In this study, the spacing was set to 20 mm. This is normally enough for UHF RFID antennas, as the whole antenna can be sintered at once.



Fig. 1. Xenon Sinteron 2010-L photonic sintering system.

### III. MANUFACTURING OF UHF RFID TAGS

The parameters for both manufacturing steps, inkjet printing and sintering, need to be optimized to produce homogenous and highly conductive structures to form high quality antennas. The optimization of these parameters is strictly case-related, depending on the chosen ink and substrate material, as well as the inkjet printing and sintering equipment.

In this study, both silver and copper nanoparticle inks were studied. We used Harima NPS-JL silver nanoparticle ink (with particle sizes of 5-12 nm and a maximum achievable resistivity of 4-6  $\mu\Omega\cdot\text{cm}$ ) and ANI Cu-IJ70 copper nanoparticle ink (with particle sizes of 10-200 nm and a maximum achievable resistivity of 5-7  $\mu\Omega\cdot\text{cm}$ ) [8, 9]. They were inkjet-printed onto 50  $\mu\text{m}$  thick polyimide (PI) substrate (Dupont<sup>TM</sup> Kapton<sup>®</sup>) with Fujifilm Dimatix DMP-2831 inkjet printer, equipped with 10  $\square\text{pl}$  print head nozzles. Kapton is a low-loss PI film, which provides a smooth, heat-resistant surface for high precision inkjet printing. Thus, it is optimal to be used in this study.

For the chosen substrate material, the printing quality was affected by the temperature of the ink cartridge and the platen, jetting voltage and jetting frequency, as well as the pattern

resolution. Among these parameters, pattern resolution is the most crucial one. To ensure that the ink droplets jetted to the polyimide substrate attach well on the substrate surface, without unnecessary spreading, we did preliminary test on droplets. A microscope image of silver nanoparticle ink droplets is shown as an example in Fig. 2; the droplet diameter of silver ink on PI was about 86  $\mu\text{m}$ , so we chose 635 dpi as the resolution, meaning the drop spacing is approximately the radius of the droplet, 40  $\mu\text{m}$ . Similar preliminary study was done for the inkjet printing parameters of the copper ink. The platen temperature was chosen quite high in the equipment, 56 °C (60 °C is the maximum). A high temperature helps ink to form a uniform surface and to dry faster. Based on the results of our preliminary tests, the actual printing parameters were chosen to be the ones listed in TABLE I. The thickness of the ink layer depends on the printing direction line width of the conductor, and, therefore, thickness varies significantly in a given sample in different areas, as presented in [10].

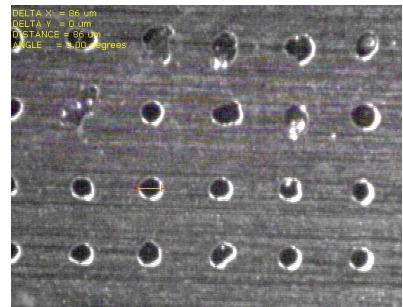


Fig. 2. Drop size test of silver nanoparticle ink on PI, droplet diameter is about 86  $\mu\text{m}$ .

After finding the inkjet printing parameters, the parameters for photonic sintering were studied. The lamp voltage was changed from 1800 V to 3000 V, with a step of 50 V, while the pulse width was fixed to 2000  $\mu\text{s}$ , which is the maximum allowed duration in equipment specifications. Also the number of needed flash pulses was studied; we did preliminary tests with 1, 2, 5, 10 and 20 pulses. The sintering results were primarily evaluated by sheet resistance measurements of inkjet-printed simple 5 mm x 50 mm line patterns (see Fig. 3).

The silver ink line pattern became fully sintered with a lamp voltage of 3000 V and two flash pulses were needed. Lower energy resulted as higher resistance while higher energy (more flash pulses) did not reduce the resistance. Photonic sintering of the copper ink was significantly more challenging than photonic sintering of the silver ink. The copper ink was successfully sintered with a single flash pulse of 2500 V. The printed trace was partially sintered when the lamp voltage was lower and the surface became more uneven when sintered with a higher voltage.

After inkjet printing and photonic sintering of these line patterns, we measured their resistances using Fluke 111 True RMS multimeter. The resistances were measured by placing the measurement probes on the opposite corners of the line pattern. The resistances are presented in TABLE II. Based on these results, as well as based on the results achieved in [3, 10], we chose to use three layers of ink in both cases. One layer

was not enough, especially with silver nanoparticle ink. The inks had different structures and this is probably causing the differences in the resistance measurement results of one-layer structures. Microscope images of three-layer sample surfaces after photonic sintering are shown in Fig. 4.

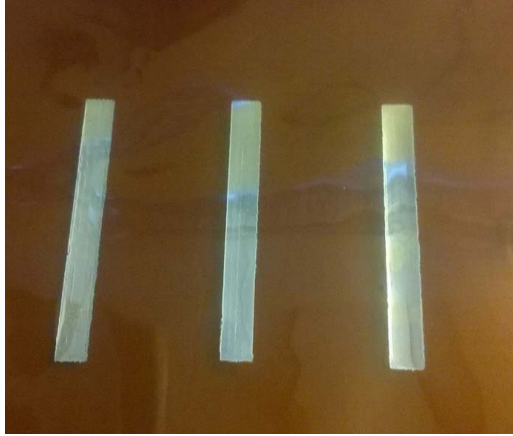


Fig. 3. Silver nanoparticle ink line patterns on PI for parameter optimization.

TABLE I. OPTIMIZED INKJET PRINTING PARAMETERS

	Silver ink	Copper ink
Cartridge temperature (°C)	28	28
Platen temperature (°C)	56	56
Jetting voltage (V)	28	25
Jetting frequency (kHz)	23	23
Pattern resolution (dpi)	635	726

TABLE II. RESISTANCES OF MANUFACTURED LINE PATTERNS

Ink	Number of ink layer(s)	Substrate	Resistance ( $\Omega$ )
Silver	1	PI	2
Silver	3	PI	0,8
Copper	1	PI	1,6
Copper	3	PI	1

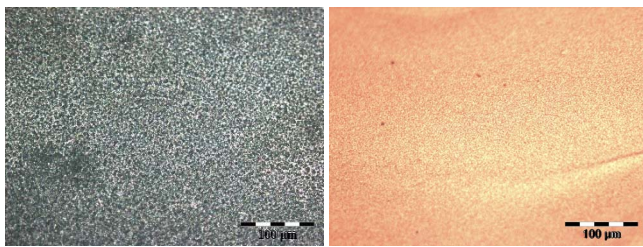


Fig. 4. Optical microscope images of manufactured three-layer silver (left) and copper (right) samples.

After finding the optimal parameters for manufacturing, we manufactured the prototype UHF RFID tags antennas. The

UHF RFID tag antenna geometry applied in this study is shown with a manufactured prototype tag in Fig. 5. This geometry represents a typical dipole antenna layout for passive UHF RFID tags and it has been already successfully used in [10]. Three-layer tag antennas were inkjet printed with silver and copper nanoparticle inks on polyimide substrate with the optimized printing parameters. The antennas were sintered using optimized photonic sintering parameters. The tag IC used in this study is NXP UCODE G2iL series IC [11]. The manufacturer had mounted the IC on a strap. The strap was attached to each tag antenna with conductive silver epoxy resin to form a fully functional passive UHF RFID tag.

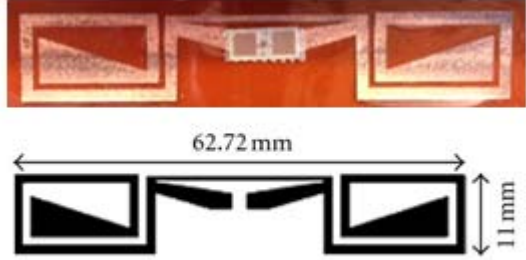


Fig. 5. Bottom: utilized tag antenna geometry. Top: a prototype of inkjet-printed and photonically sintered UHF RFID tag using copper nanoparticle ink.

#### IV. MEASUREMENTS

The prototype inkjet-printed UHF RFID tags were evaluated with Tagformance RFID measurement unit. The core operations are performed with a vector signal analyzer. Two key properties of passive UHF RFID tags were measured: threshold power and theoretical read range. Both quantities can be measured as a function of transmit frequency or as a function of tag to reader antenna angle at a point frequency. Threshold power describes the minimum transmit power, at the transmit port, to activate the tag and can be expressed as:

$$P_{TS} = \frac{P_{IC}}{G_{tx}G_{tag}\tau\left(\frac{\lambda}{4\pi d}\right)^2 |p_{tx}^\wedge \cdot p_{tag}^\wedge|^2} \quad (1)$$

where  $P_{IC}$  is the sensitivity of the RFID IC,  $G_{tx}$  and  $G_{tag}$  are the gains of the reader and tag antenna,  $\tau$  is the power transmission coefficient,  $d$  is the distance between the tag and reader antenna,  $p_{tx}^\wedge$  and  $p_{tag}^\wedge$  the unit electric field vectors of the transmitting antenna and tag antenna. The inner product of the electric field vectors describes the power loss due to possibly mismatched polarization planes between the reader and tag antenna.

Theoretical read range describes the maximal distance between the tag and reader antenna in an environment without reflections or external disturbances. The Tagformance measurement system is able to calculate the theoretical read range of a tag using its measured threshold power along with the measured forward losses. The forward loss describes the link loss between the generator's output port to the input port of an equivalent isotropic antenna placed at the tag's location. The forward loss from the transmit port to the tag is calculated

using a reference tag during the calibration procedure of Tagformance. Theoretical read range is calculated assuming that the read range is limited by the maximal allowed transmitted power levels and can be calculated as:

$$d_{Tag} = \frac{\lambda}{4\pi} \sqrt{\frac{EIRP}{P_{TS}L_{fwd}}}, \quad (2)$$

where  $\lambda$  is the wavelength transmitted from the reader,  $EIRP$  is the maximum equivalent isotropically radiated power allowed by local regulations, 3.28 W in Europe,  $P_{TS}$  and  $L_{fwd}$  are the measured threshold power and forward losses correspondingly.

The theoretical read ranges for three-layer tags are shown in Fig. 6 and the threshold power results are shown in Fig. 7. The prototype three-layer silver tags reached peak read ranges of 5.5 meters and the three-layer copper tags showed peak read ranges of 3.6 meters. The read range results of these silver tags agree with those achieved in [10], where the same inkjet-printed silver tag antenna was fabricated, though with heat sintering.

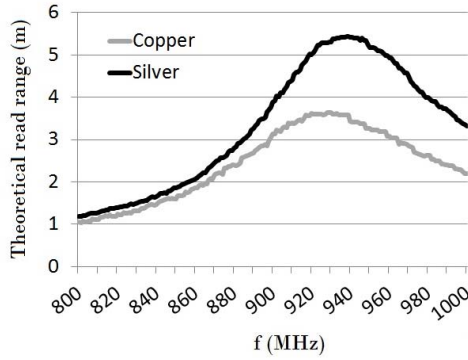


Fig. 6. Measured read ranges of inkjet-printed UHF RFID tags.

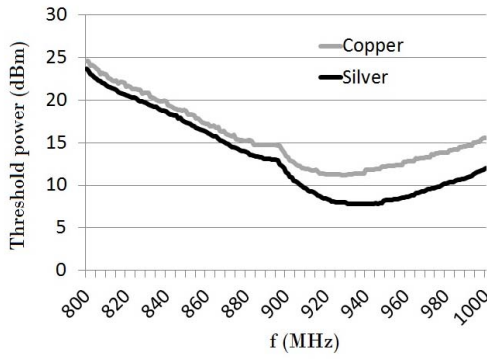


Fig. 7. Measured threshold powers of inkjet printed UHF RFID tags.

## V. CONCLUSION

In this study, we manufactured UHF RFID tags with optimized inkjet-printing and photonic sintering parameters.

First, we studied the optimal printing and sintering parameters for both silver and copper nanoparticle inks and then manufactured prototype UHF RFID tag antennas on flexible polyimide substrate. The achieved peak read range depends on the ink type and the number of printed layers. With three printed layers of silver nanoparticle ink and by efficient flash lamp sintering, read ranges of 5.5 meters were achieved. Even though the results are very promising, a lot of research work is still needed as each substrate needs its own optimized manufacturing parameters. Also, use of new ink materials, such as nickel nanoparticle ink, can provide even more possibilities for the UHF RFID technology. In addition, selective ink deposition could be used to significantly reduce the amount of conductive ink and time by identifying areas with high surface current densities and applying additional nanoparticle ink onto such areas.

## REFERENCES

- [1] L. Yang , A. Rida , R. Vyas, and M. M. Tentzeris, "RFID tag and RF structures on paper substrates using inkjet-printingtechnology", IEEE Trans. Microw. Theory Tech., vol. 55, no. 12, pp.2894 -2901, December 2007.
- [2] J. Virkki, J. Virtanen, L. Sydanheimo, L. Ukkonen, and M. M. Tentzeris, "Embedding inkjet-printed antennas into plywood structures for identification and sensing", Proc. IEEE RFID-TA, pp.34-39, November 2012.
- [3] J. Virtanen, T. Björnin, L. Ukkonen, K. Kaija, T. Joutsenoja, L. Sydänheimo, and A. Z. Elsherbeni, "The effect of conductor thickness in passive inkjet printed RFID tags," Proc. IEEE APSURSI, pp. 1-4, July 2010.
- [4] H. S. Kim, S.R. Dhage, D.E. Shim, and H.T. Hahn, "Intense pulsed light sintering of copper nanoink for printed electronics," Applied Physics A, vol. 97, no. 4, pp. 791-798, August 2009.
- [5] B. Polzinger, F. Schoen, V. Matic, J. Keck, H. Wilcke, W. Eberhardt, and H. Kueck, "UV-sintering of inkjet-printed conductive silver tracks," Proc. IEEE NANO, pp. 201-204, August 2011.
- [6] K. A. Schroder, S. C. McCool, and W. F. Furlan, "Broadcast photonic curing of metallic nanoparticle films", Proc. Nanotech, vol. 3, Chapter 2, pp.198 -201, 2006.
- [7] Xenon Sinteron 2010-L. Installation and User Manual. Xenon Corporation, June 2013.
- [8] Harima, NPS-JL Silver Nanoparticle Ink, NanoPaste Series, Metal Paste for Thin Film Formation, Datasheet, <http://www.harima.co.jp/en/products/pdf/16-17e.pdf> (13.8.2014)
- [9] Applied Nanotech Holdings, Inc, Cu-IJ70 Copper nanoparticle Ink, [http://www.appliednanotech.net/tech/conductive\\_ink\\_cu.php](http://www.appliednanotech.net/tech/conductive_ink_cu.php) (19.8.2014)
- [10] J. Virtanen, J. Virkki, A. Z. Elsherbeni, L. Sydänheimo, and L. Ukkonen, "A selective ink deposition method for the cost-performance optimization of Inkjet-Printed UHF RFID tag antennas", Int J Antennas Propag, vol. 2012, Article ID 801014, 9 pages, 2012.
- [11] NXP UCODE G2iL IC Datasheet, [http://www.nxp.com/documents/data\\_sheet/SL3S1203\\_1213.pdf](http://www.nxp.com/documents/data_sheet/SL3S1203_1213.pdf) (13.8.2014)